The Research Council of Norway (NFR)

NORSAR

NORSAR Scientific Report No. 2-93/94

Semiannual Technical Summary

1 October 1993 – 31 March 1994

Kjeller, May 1994

7.4 Some improvements of the detector / SigPro - system at NORSAR

Introduction

In operating the GERESS array, the Institute of Geophysics at the Ruhr-University of Bochum, Germany uses NORSAR software for analyzing the GERESS data. Due to special site conditions and a slightly different configuration of GERESS relative to the small aperture arrays in Scandinavia the application of the NORSAR software for GERESS data needed several adaptations. A systematic comparison of events defined by the automatic RONAPP system and events reported by international data centers led to the conclusion that many events were not located because the installed detector missed a lot of clearly visible S-type onsets (i.e. Sn, Sg, Lg, or Rg). This occurred when on all vertical beams (i.e., beams formed using vertical component sensor data only) these S-type onsets showed a relative small signal to noise ratio (SNR) relative to the P-phases and when the S-energy on the calculated incoherent beams using the horizontal components was smeared out instead of being concentrated. This observation led to a general modification of the detector for S-type onsets at the GERESS data center in Bochum using the horizontal components. After changing the detector in Bochum about 20% more events could be located by the automatic processing.

These modifications have now been implemented for the processing of GERESS data at NORSAR, and the same detector extensions have been tested for ARCESS and NORESS. Also for these two arrays, an improvement of the detection capabilities for S-type onsets can be observed using the new beam configurations.

In a separate study, the effect of the length of the analysis time window for the automatic fk-estimation and the effect of prefiltering the signal traces before estimating the fk-spectra were investigated. This study takes into account the different apertures of the arrays, and for all the arrays (ARCESS, FINESS, GERESS, and NORESS) an improvement of the automatic fk-results can be observed.

Coherent beams of rotated horizontal components

To detect S-phases on the horizontal components, one has to be aware that amplitudes and polarities of S-phases normally show large differences on the two horizontal components. The signal form of S-phases depends on the backazimuth of the incoming wave field, which defines the amplitude split into the two horizontals and it depends on the S-phase radiation pattern of the source, which defines the polarization of the S-onset. If the SV-radiation from the source in the direction of the observing station is relatively large, an S-phase is mostly visible on the radial and vertical components. These onsets are normally well detected by the installed beams that use the vertical components. In the case of a relatively large SH-radiation and a weak SV-radiation in the direction to the station the S-phase is mostly visible on the transverse component, and a signal may go undetected on both the coherent and the incoherent beam of vertical components.

To obtain the best SNR - especially for SH-onsets - the horizontal components must be rotated to their radial and transverse components, respectively. These rotated traces can then be used separately for further investigations. For ARCESS and NORESS, four 3-component stations are available for calculation of coherent beams with the rotated components. For GERESS, five 3-component stations are available. To form the beams, a mean S-velocity of 4 km/sec and several narrow band filters are used. The rotation angle is always the same as the assumed backazimuth for calculating the beam. Additionally, to detect weak S-type onsets with no preferred polarization (i.e. SH and SV show similarly small amplitudes) incoherent beams of the horizontal components for a phase velocity of 4 km/sec and different backazimuths are calculated. The new defined horizontal beams, which extend the old beam tables at NORSAR for ARCESS, GERESS, and NORESS are given in Table 7.4.1.

Fig. 7.4.1 shows two histograms of observed regional phases (velocity $\leq$ 12 km/sec) with and without the new beam tables. This result consists of 5 days (DOY 144-149, 1994) of data processing for ARCESS, GERESS, and NORSAR. The total increase of detections in this velocity range is obvious (55.6%), especially (and as expected) for velocities lower than 5 km/sec. To assess the contributions from the added detections, the whole event processing cycle (SigPro) was carried out and compared with the results of the current automatic processing at NORSAR (i.e., based on the beam tables without the new beams):

For DOY 98-100 and 104-107 in 1994, the GBF routine for multiple station phase association and event location (Ringdal and Kværna, 1989) was rerun with the new detections. Comparing the results with the original GBF locations, 13.3% more events (478 instead of 422) could be defined and the mean number of associated phases to an event increased (e.g. for DOY 104-107 by 40.7% from 3.76 to 5.30).

But also the number of events defined using the single array RONAPP routine (NORSAR Sci. Rep. No 2-88/89) increased for all 3 arrays by 18.6%. Table 7.4.2 gives the results for each array individually for the investigated 17 days (DOY 98-100, 104-107, 133-136, 144-149, 1994) and in Fig. 7.4.2 event locations are given for both the old and the new beam tables. Especially for the known source regions around the arrays the increase of new events is obvious and it is also clearly seen that the observable scatter of poorly located events at larger distances from the arrays has decreased.

To demonstrate the advantage of the new beam tables Fig. 7.4.3a shows as an example an event in southern Norway observed at NORESS, with an epicentral distance of about 250 km (March 14, 1994, 16:02). This event was not locatable because the Lg-phase was not detected with the old beam deployment. Fig. 7.4.3b shows results of the detector process using the new beam tables. At the top the two beams are seen with which the event could be defined, using the detection beam N077 of the P-phase (as in the old beam table) and the newly defined coherent beam NT13 using the transverse components (for definition see Table 7.1.1). Additionally, the SNR-traces of 3 detector beams related to S-phases are shown. It is clearly seen that the Lg-onset has the strongest and sharpest onset on the SNR-trace of beam NT13. The two other SNR-traces correspond to the formerly defined incoherent beams NH02 and NV04 which have the highest SNR for this Lg-onset. NH02

uses all 8 horizontal components and NV04 uses 8 vertical traces (A0, C-ring) as data. Note that the theoretical SNR increase by 8 traces should be higher than by 4 traces, but the SNR on the new beam NT13 is 1.7 to 2.0 times larger than on the incoherent beams.

We also observe that the onset times of S-phases can often be measured more precisely on the new beams than on the vertical beams because of the higher SNR on the horizontal beams, and also because the horizontal components are less disturbed by S-P conversions and scattered energy from the P-coda.

Fk-analysis for detections on the horizontal beams

Especially in the coda of stronger P-phases when the LTA on the verticals is still high (i.e. a high detection threshold) and P to SV conversions or scattered energy arrive at the station, P-type onsets on the horizontal components may also trigger some detections. Therefore the new beams increase the number of P-phases slightly. But the number of noise detections also increases, because the influence of one single (noisy) trace is much higher in the case of only 4(5) stations used for the beam forming. To avoid erroneous fk-results for these detections, the following new rules were developed for the SigPro routine and successfully tested:

For all detections on the horizontal components a first fk-estimate is derived using all available vertical traces. In most cases this gives reliable fk-results, but not if the detection on the horizontal beams is based mostly on SH-energy or on noise at some rotated traces. In these cases, the fk-results are arbitrary, the 'rel. fk-power' - a measure of the quality of the fk-estimation - is very low, and the results cannot be accepted. In these cases, a new fk-estimation is done with the following rules:

If the 'rel. fk-power' is lower than 0.20 it is assumed that the detected energy is an S-onset which is mostly visible on the horizontal traces. Therefore, the fk-analysis is repeated for the rotated components (for radial and transverse components separately) and for the summed square root traces of all horizontal components (this helps to estimate azimuth and velocity for very weak S-onsets which are a mixture of SH and SV energy). Then beams are calculated using these three fk-results and an SNR of the detected onset is remeasured on these beams. The estimated velocity and azimuth of the beam with the highest SNR are chosen as representing this detection, but they are only accepted if the estimated velocity is an S-velocity, if the SNR is higher than the detection threshold of the beam, and if the amplitude of this onset is higher than on a beam calculated with the same parameters, but using the vertical components of the 3-component sites. If these conditions are not satisfied, this detection is classified as noise.

Improvements of the fk-analysis

From off-line fk-analysis it is known that the positioning of the time window relative to the detected onset is of high importance for quality, stability, and reliability of the fk-results. In the following, different changes of the automatic fk-analysis were tested for

ARCESS, FINESS, GERESS, and NORESS. For all tests of new parameter settings more than 100 fk-analyses including different phase-velocities and frequency ranges were compared. The mean of the 'rel. fk-power' - a measure of the quality of the fk-analysis - was used to decide on the success of different parameter settings.

At the moment, the automatic fk-analysis at NORSAR uses a constant time window of 3 sec starting 0.5 sec before the estimated onset time. We can assume that the first cycles of an onset are the most coherent part of this signal. The chosen time window of 3 sec is quite appropriate for signals with a dominant period of about 1 Hz. But for more high frequent signals a 3 sec long time window includes incoherent coda energy which can easily influence the fk-results. Therefore, a frequency dependent time window for the automatic fk-analysis was defined and tested.

With the travel time of the slowest signals (~2 km/sec) crossing an array of aperture a and with the dominant period T_s measured during the onset time estimation, the length t_w of the fk-analysis time window was defined as

$$t_w = 2 * T_s + a / 2$$

This time window guarantees that at least two cycles of the signals are within the fk-analysis window for each channel. Using this time window as a guide-line, several minimum and maximum values of the fk-time window were tested. Another parameter which was varied was the time length the fk-time window starts before the estimated onset. It was found that this value must be increased slightly in the case of GERESS due to the larger aperture of this array. The time window limits with the best fk-results are given for each array in Table 7.4.3.

Additionally, it was found that the fk-results became more reliable when using prefiltered data. The reason for this is that large amplitudes outside the interesting frequency range (especially low frequent noise) can affect the fk-analysis, which uses small time windows for Fourier- transformation. Therefore the traces were prefiltered with a slightly wider pass band (+/- 20%) than the pass band used for the detecting beam.

To avoid erroneous fk-results from the numerous detections of the Glomma river Rg-noise (Kværna, 1990) in the vicinity of NORESS, two beams to detect this noise were tested successfully. These 'negative' detections can now be thrown out to reduce unwanted associations in the event processing routines, in similarity to the two beams especially formed for two know sources of acoustical noise at GERESS.

The advantage of these new rules is demonstrated as follows. For 5 days (DOY 144 - 149, 1994) a total number of 6154 new fk-results from all investigated arrays could be compared with the original NORSAR SigPro results. Fig. 7.4.4 shows 6154 differences of the 'rel. fk-power' for the new and the old SigPro recipes plotted against the dominant frequency of the onsets (Fig. 7.4.4a), and plotted against the estimated ray parameter of the onset (Fig. 7.4.4b). The size of the symbols corresponds to the number of hits for this value, respectively. The figures clearly show that the 'rel. fk-power' increase by 9.5% over the whole frequency range of analyzed signals and also for all ray parameters. Finally, Fig. 7.4.5 shows for all 6154 compared fk-results the new 'rel. fk-power' values against the cor-

responding original 'rel. fk-power' values. It is clearly visible that especially for onsets with small 'rel. fk-power' using the old recipes the quality increases significantly, i.e., the fk-results for weak onsets became more stable and reliable.

Conclusions

The investigated extensions of the beam tables for ARCESS, GERESS and NORESS using coherent beams of rotated horizontal components clearly increase the S-phase detection capabilities of these arrays, especially in the case of relatively strong SH-wave radiation from the source to the array. Therefore, the new beams also led to a larger number of events defined and located by automatic processes (e.g. RONAPP and GBF).

The tested changes of the automatically chosen time window (i.e. length and position relative to the estimated onset time) for the fk-analysis and prefiltering the single traces stabilized the fk-results. For ARCESS, FINESS, GERESS, and NORESS the 'rel. fk-power' increases in the mean and especially the erroneous estimates of phase velocity and azimuth based on fk-results with very low 'rel. fk-power' could be reduced. This also improves the results of the automatic data analysis for all kinds of seismic phases.

J. Schweitzer

References

Kværna, T. (1990): Sources of short-term fluctuations in the seismic noise level at NORESS. *Phys. Earth Planet. Int.* 63, 269-276.

Ringdal, F. and T. Kværna (1989): A multichannel processing approach to real time network detection, phase association and threshold monitoring. *Bull. Seism. Soc. Amer.* 79, 1927-1940.

BEAM	AZ deg	VEL km/sec	FILTER Hz - Hz	ORD	THR	STATION LIST	COMMENTS
New horizontal beams added to the old beam table of ARCESS (NORSAR Sci. Rep. No. 1-89/90):							
FR01 - FR12	*	4.0	0.7- 2.0	4	3.8	A0_sr C1_sr C4_sr C7_sr	radial components
FR13 - FR24	*	4.0	3.5- 5.5	3	3.5	A0_sr C1_sr C4_sr C7_sr	radial components
FR25 - FR36	*	4.0	2.0- 4.0	3	3.5	A0_sr C1_sr C4_sr C7_sr	radial components
FS01 - FS12	*	4.0	3.5- 5.5	3	3.0	A0_sn A0_se C1_sn C1_se C4_sn C4_se C7_sn C7_se	incoherent horizontals
FS13 - FS24	*	4.0	1.0- 4.0	3	3.0	A0_sn A0_se C1_sn C1_se C4_sn C4_se C7_sn C7_se	incoherent horizontals
FS25 - FS36	*	4.0	5.0-10.0	3	3.0	A0_sn A0_se C1_sn C1_se C4_sn C4_se C7_sn C7_se	incoherent horizontals
FT01 - FT12	*	4.0	0.7- 2.0	4	3.8	A0_st C1_st C4_st C7_st	transverse components
FT13 - FT24	*	4.0	3.5- 5.0	3	3.5	A0_st C1_st C4_st C7_st	transverse components
FT25 - FT36	*	4.0	2.0- 4.0	3	3.5	A0_st C1_st C4_st C7_st	transverse components
New horizontal beams added to the old beam table (as running at NORSAR since DOY 123, 1991) of GERESS:							
GR01 - GR12	*	4.0	0.7- 2.0	4	3.5	A2_sr C2_sr D1_sr D4_sr D7_sr	radial components
GR13 - GR24	*	4.0	1.0- 3.0	4	3.5	A2_sr C2_sr D1_sr D4_sr D7_sr	radial components
GR25 - GR36	*	4.0	2.0- 4.0	3	3.5	A2_sr C2_sr D1_sr D4_sr D7_sr	radial components
GS01 - GS12	*	4.0	0.7- 2.0	4	3.0	A2_sn A2_se C2_sn D2_se D1_sn D1_se D4_sn D4_se D7_sn D7_se	incoherent horizontals
GS13 - GS24	*	4.0	1.0- 4.0	3	3.0	A2_sn A2_se C2_sn D2_se D1_sn D1_se D4_sn D4_se D7_sn D7_se	incoherent horizontals
GS25 - GS36	*	4.0	6.0-10.0	3	3.0	A2_sn A2_se C2_sn D2_se D1_sn D1_se D4_sn D4_se D7_sn D7_se	incoherent horizontals
GT01 - GT12	*	4.0	0.7- 2.0	4	3.5	A2_st C2_st D1_st D4_st D7_st	transverse components
GT13 - GT24	*	4.0	1.0- 3.0	4	3.5	A2_st C2_st D1_st D4_st D7_st	transverse components
GT25 - GT36	*	4.0	2.0- 4.0	3	3.5	A2_st C2_st D1_st D4_st D7_st	transverse components
New horizontal beams added to the old beam table of NORESS (NORSAR Sci. Rep. No. 1-89/90):							
N998	100	2.8	2.0- 3.0	2	3.5	all sz	Glomma noise (Kvaerna, 1990) beam
N999	100	2.8	3.0- 4.0	2	3.5	all sz	Glomma noise (Kvaerna, 1990) beam
NR01 - NR12	*	4.0	0.7- 2.0	4	3.8	A0_sr C1_sr C4_sr C7_sr	radial components
NR13 - NR24	*	4.0	3.5- 5.5	3	3.5	A0_sr C1_sr C4_sr C7_sr	radial components
NR25 - NR36	*	4.0	2.0- 4.0	3	3.5	A0_sr C1_sr C4_sr C7_sr	radial components
NS01 - NS12	*	4.0	3.5- 5.5	3	3.0	A0_sn A0_se C1_sn C1_se C4_sn C4_se C7_sn C7_se	incoherent horizontals
NS13 - NS24	*	4.0	1.0- 4.0	3	3.0	A0_sn A0_se C1_sn C1_se C4_sn C4_se C7_sn C7_se	incoherent horizontals
NS25 - NS36	*	4.0	5.0-10.0	3	3.0	A0_sn A0_se C1_sn C1_se C4_sn C4_se C7_sn C7_se	incoherent horizontals
NT01 - NT12	*	4.0	0.7- 2.0	4	3.8	A0_st C1_st C4_st C7_st	transverse components
NT13 - NT24	*	4.0	3.5- 5.0	3	3.5	A0_st C1_st C4_st C7_st	transverse components
NT25 - NT36	*	4.0	2.0- 4.0	3	3.5	A0_st C1_st C4_st C7_st	transverse components

*

BEAM-	AZ	BEAM-	AZ	BEAM-	AZ
01 =	0 deg	13 =	0 deg	25 =	0 deg
02 =	30 deg	14 =	30 deg	26 =	30 deg
03 =	60 deg	15 =	60 deg	27 =	60 deg
04 =	90 deg	16 =	90 deg	28 =	90 deg
05 =	120 deg	17 =	120 deg	29 =	120 deg
06 =	150 deg	18 =	150 deg	30 =	150 deg
07 =	180 deg	19 =	180 deg	31 =	180 deg
08 =	210 deg	20 =	210 deg	32 =	210 deg
09 =	240 deg	21 =	240 deg	33 =	240 deg
10 =	270 deg	22 =	270 deg	34 =	270 deg
11 =	300 deg	23 =	300 deg	35 =	300 deg
12 =	330 deg	24 =	330 deg	36 =	330 deg

Table 7.4.1. List of newly tested horizontal beams to extend the former beam tables of ARCESS, GERESS, and NORESS.

Array	No. of Events		
	Old Beam Table	New Beam Table	Increase %
ARCESS	368	418	13.6
GERESS	288	372	29.2
NORESS	155	172	11.0
	811	**962**	**18.6**

Table 7.4.2. Number of located events by the single array RONAPP process (NORSAR Sci. Rep. No 2-88/89), for the old and for the new beam tables, respectively, for a total of 17 days (DOY 98-100, 104-107, 133-136, 144-149).

Array	Aperture (km)	Min. Time Window (sec)	Max. Time Window (sec)	Start Time before Onset (Sec)
ARCESS	3.0	1.75	2.50	0.50
FINESS	2.0	2.00	2.50	0.50
GERESS	4.0	2.0	3.50	0.75
NORESS	3.0	1.75	2.50	0.50

Table 7.4.3. Parameters for setting the frequency dependent fk-time window for the investigated arrays in order to obtain the highest 'rel. fk-power'.

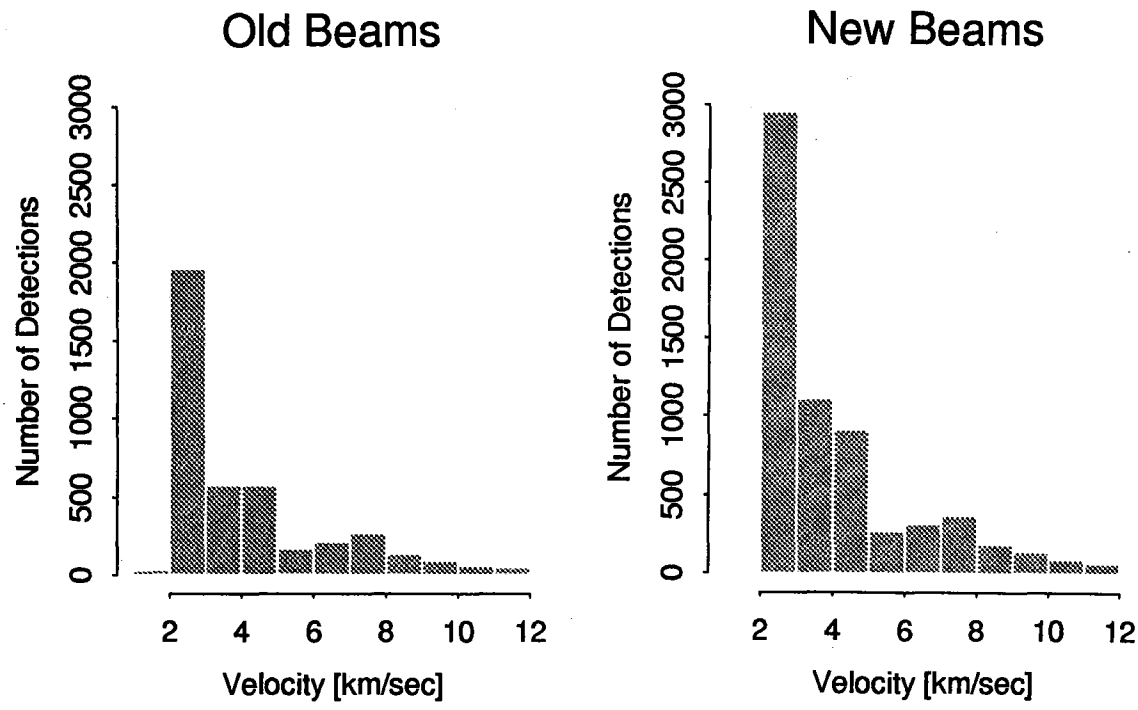

Fig. 7.4.1. Number of observed phases vs. the estimated velocities for the old and the new beam tables. The histograms show the results for ARCESS, GERESS, and NORESS together.

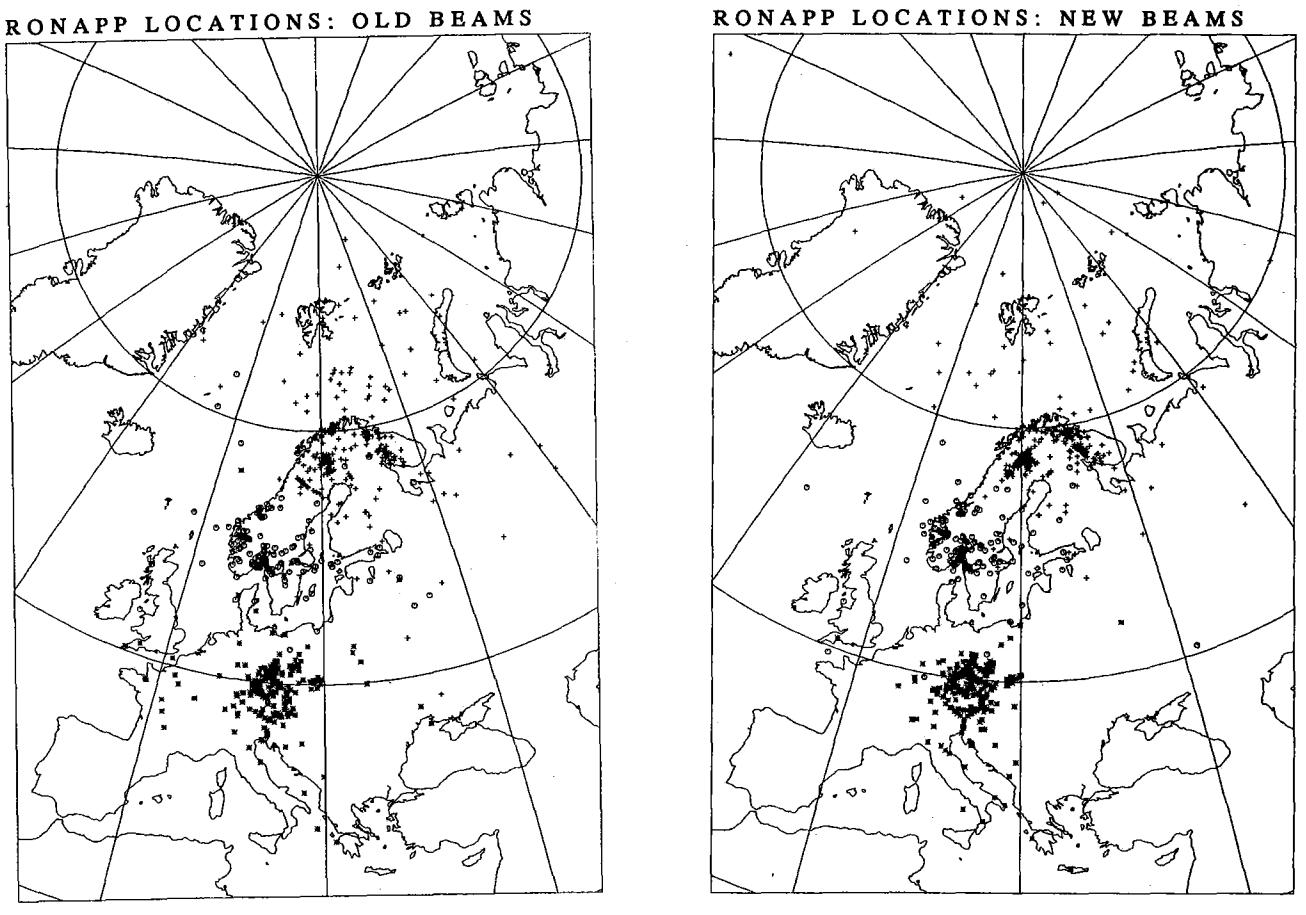

Fig. 7.4.2. Events located with the old and the new beam tables for the 17 days analyzed.

a)

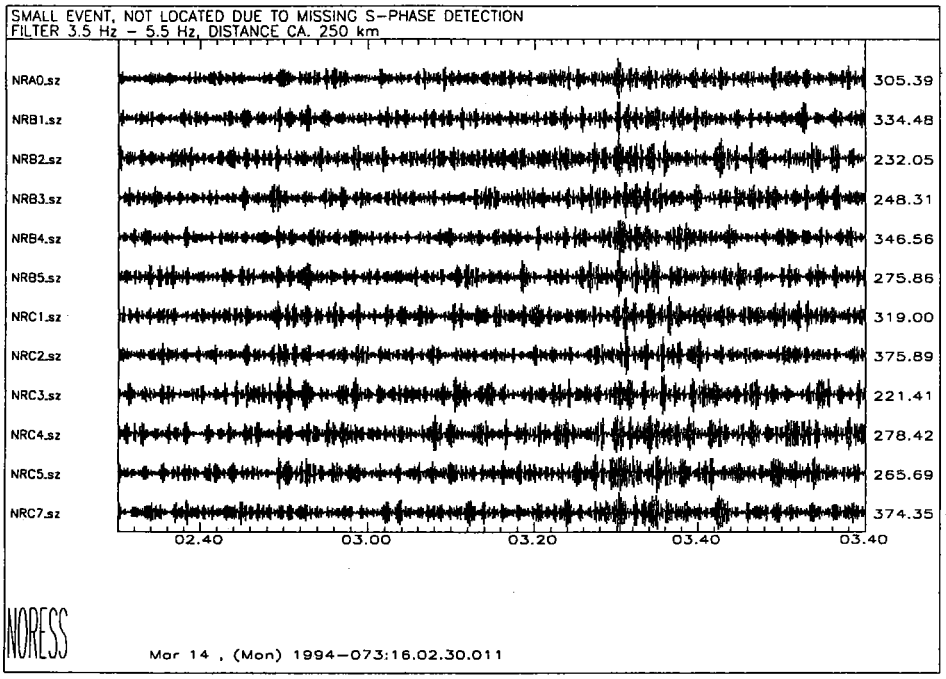

b)

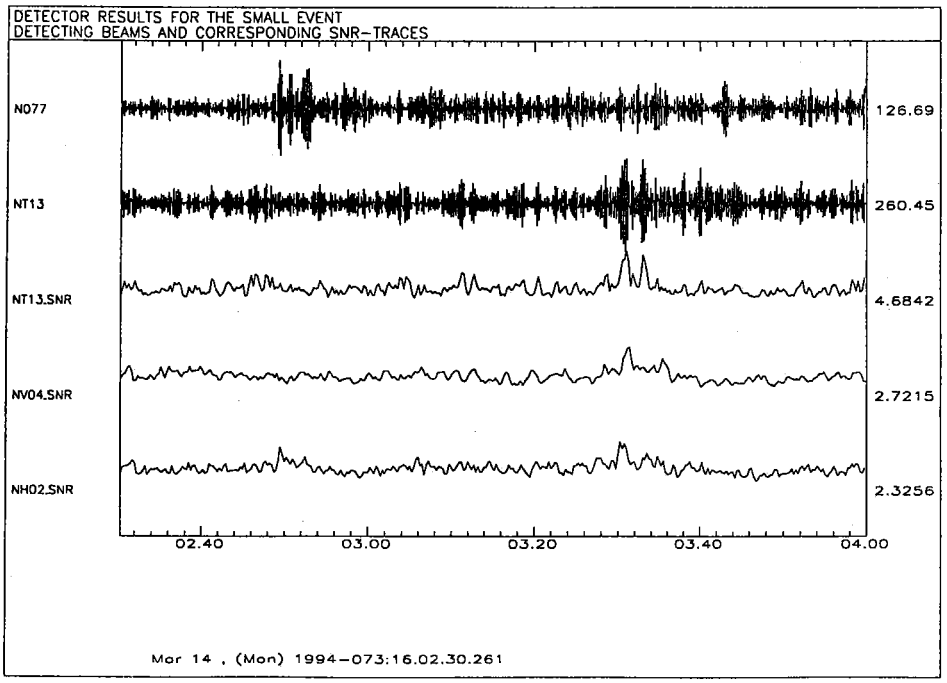

Fig. 7.4.3. An example of an event that was not locatable with the old beam set due to missing S-phase detection. A selection of band pass filtered (3.5 Hz - 5.5 Hz) single traces showing the clearly visible S-phase onset for this NORESS event (Fig. 7.4.3a). Detector beams of P-onset and S-onset and SNR-traces for several beams to detect S-phases of the discussed example (Fig. 7.4.3b).

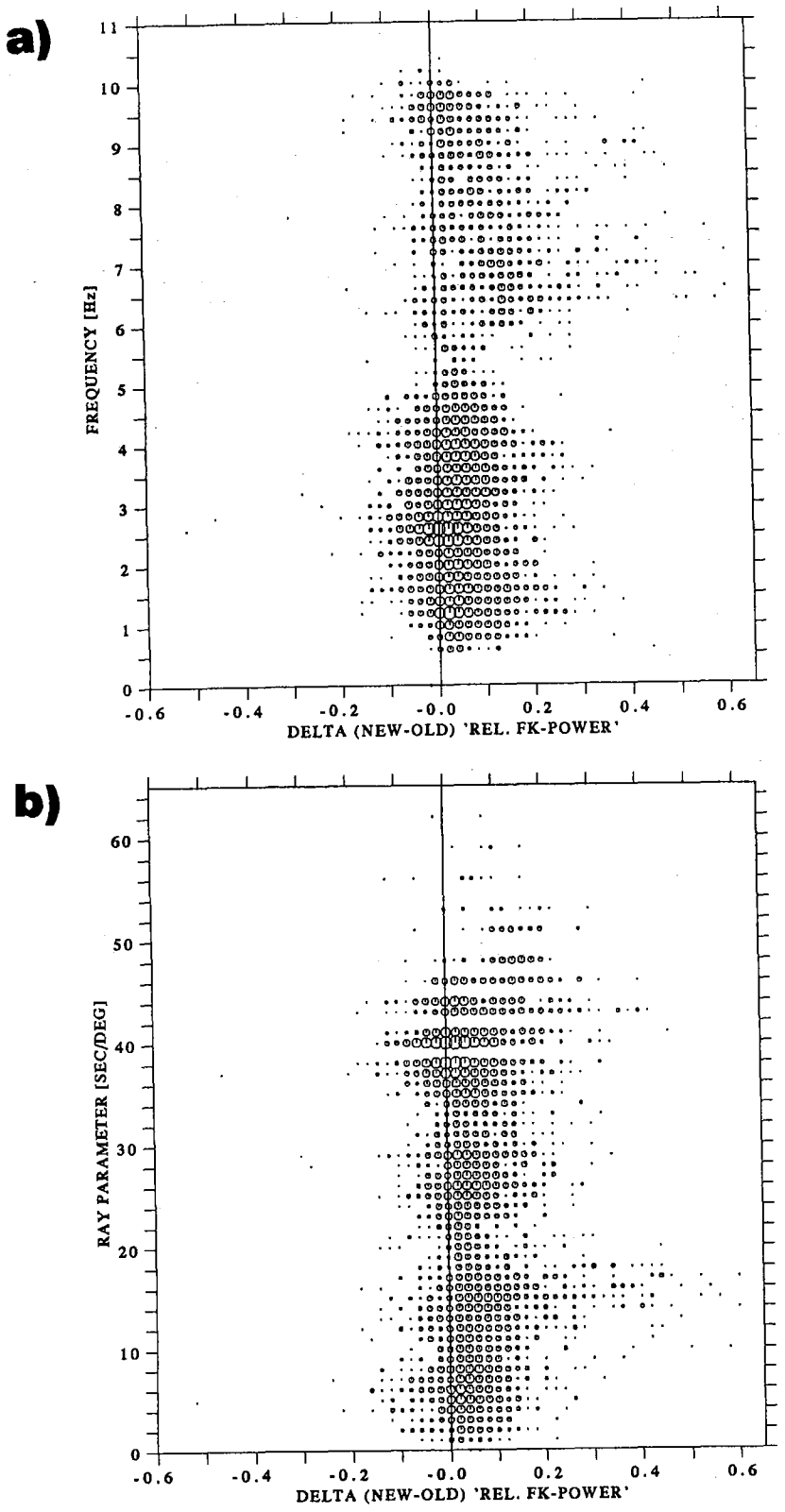

Fig. 7.4.4. Differences between the new and the old 'rel. fk-power' for 6154 estimations plotted against the signal frequency (Fig. 7.4.4a) and against the signal ray parameter (Fig. 7.4.4b).

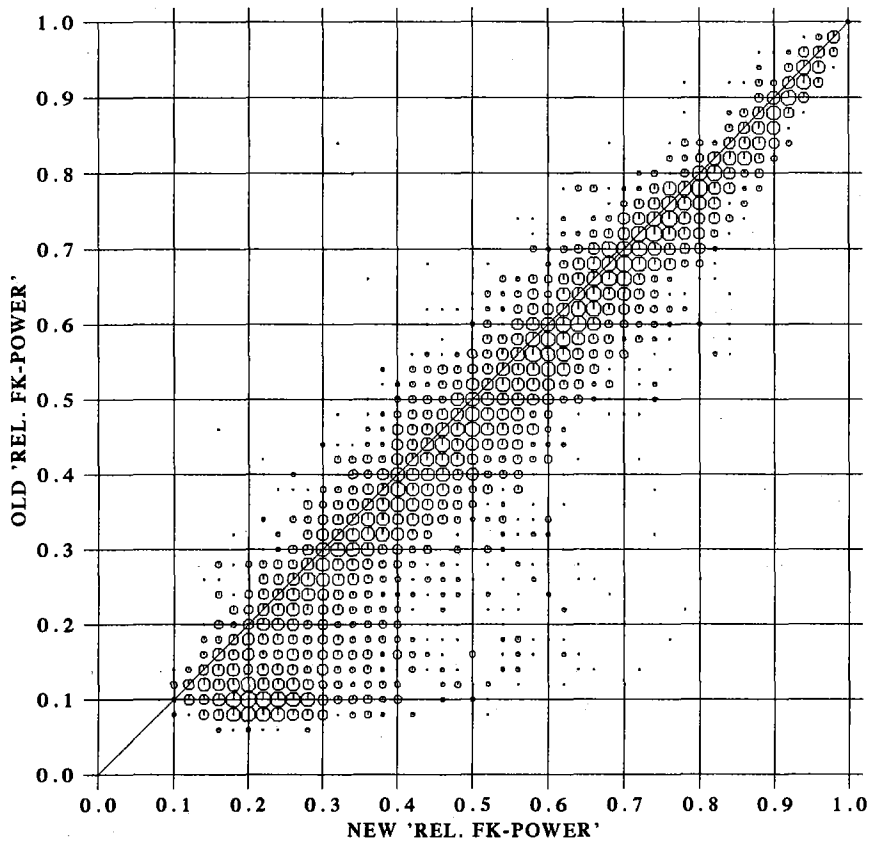

Fig. 7.4.5. New estimated 'rel. fk-power' with respect to the 'rel. fk-power' using the original recipes.